

In the first state, τ_{Σ} is dependent on the boiling processes and on the hydraulic phenomena associated with the design of the drainage tube. The transition to the second state is via thermohydraulic resonance, where the oscillation amplitude is largest. In the second state, the oscillations are governed by the liquid boiling only in the vapor-generating tubes. As P_c increases, there is a monotone decrease in the oscillation intensity and period. In the third state (with $P_c/P_{cr} \geq 0.2 = 0.3$), the oscillations have practically no effect on the operation of the system or are absent completely.

LITERATURE CITED

1. A. I. Leont'ev, O. O. Mil'man, and V. A. Fedorov, *Inzh.-Fiz. Zh.*, **48**, No. 1, 5-10 (1985).
2. A. I. Leont'ev, O. O. Mil'man, and V. A. Fedorov, *Teplofiz. Vys. Temp.*, **24**, No. 2, 301-306 (1986).
3. V. V. Aleksandrov and N. G. Rassokhin, *Teploenergetika*, No. 11, 62-64 (1985).
4. A. P. Proshutinskii and A. G. Lobachev, *Teploenergetika*, No. 3, 51-55 (1979).
5. S. M. Lukomskii, P. I. Povarin, and R. I. Shneerovich, *Trudy TsKTI*, No. 101, 217-225 (1970).
6. O. N. Koban'kov and V. V. Yagov, *Teploenergetika*, No. 5, 67-68 (1980).
7. A. P. Simonenko, *Papers from Nikolaev Ship-Building Institute [in Russian]*, Issue 187 (1982), pp. 19-26.
8. O. M. Baldina, *Trudy TsKTI*, No. 62, 7-14 (1965).
9. J. Delays, M. Gio, and M. Ritmoller, *Heat Transfer and Hydrodynamics in Nuclear and Thermal Power Engineering [Russian translation]*, Moscow (1984).
10. J. Hewitt and N. Hall-Taylor, *Annular Two-Phase Flows [Russian translation]*, Moscow (1974).
11. A. I. Leont'ev, B. M. Mironov, A. D. Korneev, et al., *Trudy MVTU*, No. 195, Issue 2, 24-33 (1975).
12. B. S. Fokin, A. F. Aksel'rod, and E. N. Gol'dberg, *Inzh.-Fiz. Zh.*, **47**, No. 5, 727-731 (1984).
13. S. S. Kutateladze, *Teploenergetika*, No. 6, 54-55 (1979).

HYDRODYNAMICS OF AN ASCENDING LIQUID FILM FLOW AND VAPOR FLUX IN A VERTICAL ANNULAR CHANNEL

M. K. Bezrodnyi and Yu. V. Antoshko

UDC 536.27

Results are represented of an experimental investigation of crisis phenomena constraining different modes of an ascending liquid film flow under the action of a vapor flux on the basis of liquid film parameter measurements.

A significant quantity of papers [1-16] is devoted to investigation of the phenomenon of destruction of the stability of different flow modes of a two-phase stream in vertical channels. Meanwhile the results of investigations characterizing the stability of film flow in an ascending coflow are of limited nature [14-16]. Consequently, there are uninvestigated areas on maps of two-phase flow modes in vertical tubes and a number of characteristic transitions between the flow modes is indicated provisionally. In addition, available experimental data in the area of individual transitions between different flow modes are obtained on the basis of different methods, which makes their comparison difficult.

The available boundaries of the annular flow mode are obtained principally in a study of a descending liquid film coflow and vapor flux [5-13]. L. Ya. Zhivaikin [14] and B. I. Nigmatullin et al. [15] performed a direct experimental investigation of liquid film disruption phenomenon in a vertical ascending flow. The equations obtained that characterize the phenomenon of film rupture differ radically in structure, which is apparently explained by the determination of different physical effects in the experiments during interaction of the light phase flux and the liquid film as well as by utilization of different methodological approaches.

Investigation of the film flow modes was performed on an experimental set-up (Fig. 1) consisting of the following main components: a vapor generator chamber, a working section, a condenser, chambers for condensate collection, apparatus for fluid insertion into the annular channel of the working section, and a measuring part. The _

Kiev Polytechnic Institute. Translated from *Inzhenerno-Fizicheskii Zhurnal*, Vol. 58, No. 3, pp. 425-430, March, 1990. Original article submitted October 18, 1988.

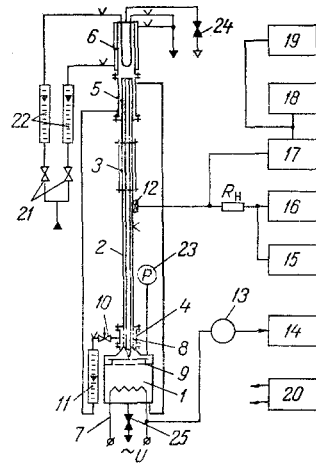


Fig. 1

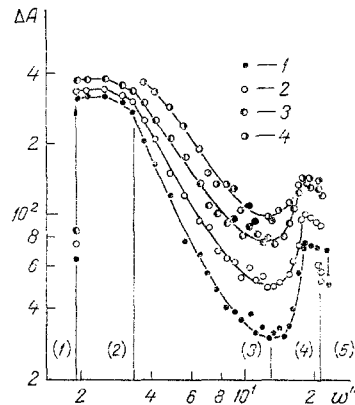


Fig. 2

Fig. 1. Diagram of the experimental set-up: 1) vapor generating chamber; 2) annular channel; 3) glass insert; 4) fluid input chamber in the annular channel; 5) condensate collection chamber; 6) condenser; 7) electrical heater; 8) porous insert; 9) separator; 10 and 21) regulating valves; 11 and 22) rotameters; 12) liquid film thickness sensor; 13) current transformer; 14) wattmeter; 15) frequency meter; 16) signal generator; 17) microvoltmeter; 18) integrating voltmeter; 19) fast-response recorder; 20) electronic thermometer; 23) manometer; 24 and 25) globe valve.

Fig. 2. Nature of the change in the mean-integral liquid film thickness as the vapor velocity grows for $Fr_{fi} < 0.1$: 1) $Q_m = 4.4 \cdot 10^{-6} \text{ m}^2/\text{sec}$, 2) $5.8 \cdot 10^{-6}$, 3) $7.4 \cdot 10^{-6}$, 4) $9.7 \cdot 10^{-6} \text{ m}^2/\text{sec}$.

working section was in the form of vertical tubes with a glass section in the upper part and a coaxially arranged blind internal insert forming an annular channel of $17 \times 10 \text{ mm}$ transverse dimensions and 2 m long. The apparatus for fluid insertion was in the form of a chamber with a porous insert matched with the outer pipe of the working section and located in the lower part of the annular channel.

The measuring part of the set-up assured measurement of the thermal power, the mass flow rate of the fluid inserted in the annular channel, the fluid film parameters, the pressure of the working medium in the vapor generating chamber. The mass flow rate of the cooling water and its temperature at the condenser input and output were also measured for thermal balance information.

The ascending two-phase flow produced because of the vapor flow going from the vapor generating chamber and the regulatable condensate flow delivered to the channel through the porous insert and entrained by the vapor in the ascending co-motion was the object of investigation. The features of the flow organization and the range of the phase consumption parameters assured mainly film flow modes with fluid film motion along the outer wall of the annular channel. In this connection the method of investigating the flow modes was constructed on the basis of studying the regularities in the change in the fluid film parameters.

The fluid film thickness in the channel was measured by an acoustic method analogous to that described in [17] and based on the dependence of the stress on the piezoceramic emitter (at a fixed excitation frequency) on the quantity of adjacent medium. As the liquid phase mass adjacent to the emitter surface grew here the stress on the emitter varied. Therefore, by measuring this stress, the nature of the change in the quantity of liquid phase, i.e., the fluid film thickness on the emitter surface mounted flush with the channel wall, could be obtained.

Application of a $8 \cdot 10^{-3} \text{ m}$ diameter emitter permitted obtaining not only the nature of the change in the mean integral thickness of the fluid film at the site of the emitter mounting but also the low-frequency structure of the film wave surface on the high-speed recorder diagram.

The investigations were performed by using freon-113 and ethanol as working fluids for a pressure change from 0.1-0.45 MPa, a $1.2 \cdot 10^{-6}$ - $90 \cdot 10^{-6} \text{ m}^2/\text{sec}$ change in the volume density of the wall spraying, and a 3-44 m/sec change in the vapor velocity. The experiments were performed by two methods: the nature of the change in fluid film thickness was investigated by the change in the stress on the piezoceramic emitter as a function of the vapor mass flow rate for

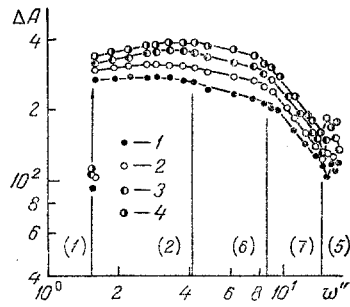


Fig. 3

Fig. 3. Nature of the change in the mean integral fluid film thickness as the vapor rate grows for $Fr_{fi} > 0.1$: 1) $q_m = 1.85 \cdot 10^{-5} \text{ m}^2/\text{sec}$, 2) $2.2 \cdot 10^{-5}$, 3) $3.75 \cdot 10^{-5}$, 4) $5.15 \cdot 10^{-5} \text{ m}^2/\text{sec}$.

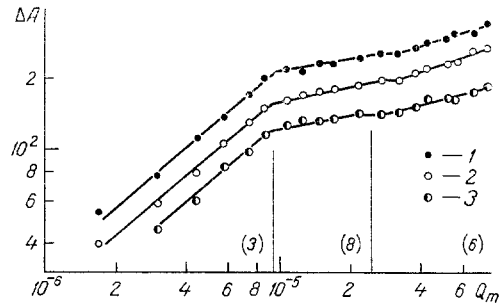


Fig. 4

Fig. 4. Nature of the change in the mean integral fluid film thickness as the channel wall spraying density grows: 1) $w'' = 4.8 \text{ m/sec}$, 2) 6.9, 3) 9.7.

a fixed fluid mass flow rate and the nature of the change in the fluid film thickness as a function of the fluid mass flow rate for a fixed vapor flow rate. The pressure in the channel was maintained constant here.

The individual flow modes of the two-phase flow were identified on the basis of a comparison of visual flow patterns, regularities of the change in the fluid film thickness parameters as a function of the vapor and fluid consumption parameters, as well as the characteristic structures of the fluid film wave surface during passage from one flow mode to another.

Figure 2 illustrates the existence of characteristic two-phase flow motion modes for relatively low values of the fluid mass flow rate (bulk spraying density Q_m) and a vapor rate change in a broad range. It is seen from the figure that for small values of the vapor rate an ascending liquid phase motion does not generally exist (mode 1). The fluid introduced into the channel here flows off downward in counterflow to the vapor. Upon the achievement of a certain critical vapor rate above the site of fluid injection, a two-phase flow is suddenly formed that exists in the form of a frothy mode and is manifest on the graph by the appearance of relatively stable values of the mean integral fluid film thickness parameter (mode 2) in the form of a stress change ΔA at the emitter. For a definite value of the vapor rate, the frothy flow vanishes spasmodically and a stable fluid film is formed on the channel wall whose thickness diminishes sharply as the vapor rate increases (mode 3). A further increase in the vapor rate results in the loss of stability of the film wave surface, as is manifested in the formation of rough waves that increase the means effective value of the fluid film thickness (mode 4). An increase in the vapor rate in this mode results in the fact that fluid rupture from the film surface occurs for a definite critical value whereupon the film thickness diminishes spasmodically to very small values. As the vapor rate increases further, the fluid motion occurs in the form of drops in flow core, i.e., a disperse flow mode takes place (mode 5).

Typical film flow characteristics are represented in Fig. 3 as a function of the vapor rate for relatively high values of the fluid mass flow rate (spraying density). As in Fig. 2, a "dry tube" mode is observed at a low vapor rate when there is no fluid in the ascending stream (mode 1). Later the frothy mode occurs in a certain range of vapor rate variation, for which the film thickness parameter grows to the maximal value (mode 2). A break in the curve with a certain subsequent diminution of the film thickness parameter indicates the onset of divided annular flow with a relatively stable fluid film (mode 6). A comparison with the corresponding mode 3 in Fig. 2 indicates the shallower nature of the film thickness dependence on the vapor rate which apparently indicates moisture transfer between the film and the stream core and characterizes the mode 6 as disperse-annular in contrast to the mode 3 (Fig. 2) as purely annular. A further increase in the vapor rate results in active phase interaction whereupon the fluid film thickness diminishes abruptly (mode 7). Upon achievement of a certain critical value of the vapor rate, the whole fluid excess in the film is separated into the vapor stream, and a very thin microfilm with a relatively smooth surface remains on the tube surface because of settling of the drops from the stream core (mode 5). Therefore, here as before (in Fig. 2), the development of the process is completed by the same phase, the disperse flow mode of a two-phase flow.

Typical characteristics are shown in Fig. 4 in the form of a dependence of the film thickness parameter on the fluid mass flow rate for fixed values of the vapor rate that assure an ascending fluid film flow. It is seen that in the domain of relatively small values of the tube spraying density the film thickness depends sufficiently strongly on the fluid mass flow rate, which also confirms the assumption about the existence of mass flow rate phase parameters of the

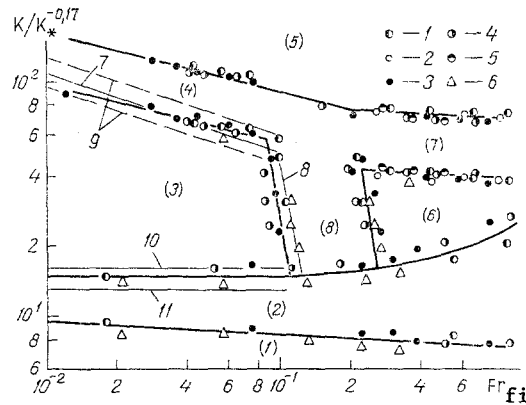


Fig. 5. Flow mode pattern: 1) counterflow; 2) emulsion; 3) annular; 5) disperse; 6) disperse-annular; 4, 7, 8) transition; 1-5) freon-113: 1) $P = 0.1$ MPa, 2) 0.15, 3) 0.2, 4) 0.3, 5) 0.4 MPa; 6) ethanol: $P = 0.1$ MPa; 7) by the Kutaleladze formula [8]; 8) from Zhivaikin data [14]; 9) [7]; 10) [2]; 11) [10, 11].

purely annular flow mode (mode 3) in this domain. For a certain critical value of the spraying density, a break is observed in the curve, the tempo of film thickness growth slows down substantially, which indicates entrainment of part of the fluid in the flow core and onset of an unstable annular flow mode (mode 8). As the fluid mass flow rate increases further, the film thickness intrinsically reaches a certain limit and the growth observable in the film thickness parameter indicates the influence of the fluid apparent mass because of the constant moisture transfer between the film and the flow core with the formation and destruction of very large waves on the phase interfacial surface. Visual observations as well as the development of a film wave surface structure permit speaking about the existence of mass flow rate parameters of the vapor and fluid of the developed disperse-annular flow mode (mode 6) in this domain.

The experimental material represented indicates a manifold of different structural flow forms of the ascending two-phase flow on the one hand, and the presence of clear enough determinable crisis transition from some flow forms to others, on the other hand, which permits going over to a generalized representation of the boundaries of variation of the flow modes and compilation of a refined pattern of ascending film flow modes.

Taking account of the crisis nature of the phenomena governing the replacement of individual flow modes of a two-phase flow, a dependence of the stability criterion of individual flow structures on the governing dimensionless parameters in the form

$$K = f \left(Fr_{fi}, Ga, We, \frac{\rho' + \rho''}{\rho'}, \frac{v'}{v''} \right) \quad (1)$$

is used in [1, 12] for the generalized representation of appropriate test data.

Analysis of the test data obtained reinforces the representativity of the generalized relationships on the basis of using a two-phase flow stability criterion. Meanwhile, a one-to-one relation exists for two-phase systems in the liquid-vapor form on the saturation line between individual parameters of (1). Moreover, it is shown in [18, 19] that the compressibility of the two-phase medium exerts substantial influence on the regularities of the crisis phenomena in similar systems, which can be taken into account by using the pressure criterion K_p . The influence of the transverse dimensions of the channel (the criterion We) is inessential according to the data of these researches. In this connection

$$K = f (Fr_{fi}, K_p) \quad (2)$$

is used to generalize the test data obtained and to construct patterns of the flow modes.

The results of generalizing the experimental data are represented in Fig. 5. There is obtained on the basis of generalization of the test data that the influence of two-phase medium compressibility on the regularity of the crisis transitions is actually taken into account sufficiently well by using the criterion K_p . The dependence of the stability criterion on K_p is observed in the band $K_p < 2 \cdot 10^4$, which corresponds to relatively small values of the two-phase medium pressure. For higher values of K_p ($K_p \geq 2 \cdot 10^4$) the regularities of the crisis replacement of flow modes are self-similar relative to the compressibility of the two-phase medium.

It follows from Fig. 5 that the method of investigation utilized as well as the generalization performed on the test data permit a sufficiently representative pattern to be obtained for the ascending flow modes in a broad range of parameters. The boundaries of all the modes noted are clearly denoted in the pattern. The comparison performed on the results obtained and known data indicates their satisfactory agreement with the individual boundaries and simultaneously explains their objective existence and physical nature in the light of a more complete pattern of characteristic film flows in an ascending two-phase flow.

NOTATION

w'' , vapor rate, m/sec; ρ' , ρ'' , fluid and vapor densities, kg/m³; ν' , ν'' , kinematic fluid and vapor viscosity coefficients, m²/sec; σ , surface tension coefficient, N/m; g , acceleration of gravity, m/sec²; l , linear dimension, m; P , pressure, MPa; δ , Laplace constant, m; ΔA , stress change on the fluid film thickness sensor, mV; Q_m , bulk spraying density, m²/sec. Criteria: $Fr_{fi} = Q_m / \delta \sqrt{g\delta}$, Froude for the fluid film; $Ga = g\delta^3 / \nu'^2$, Galileo; $We = \sigma / g(\rho' - \rho'')l^2$, Weber; $K = \omega'' \sqrt{\rho''} / \sqrt{\sigma g(\rho' - \rho'')}$, Kutateladze stability; $K_p = P\delta / \sigma$, pressure; $K_* = K_p$ for $K_p < 2 \cdot 10^4$, $K_* = 2 \cdot 10^4$ for $K_p \geq 2 \cdot 10^4$.

LITERATURE CITED

1. S. S. Kutaletadze and M. A. Styrikovich, Hydrodynamics of Gas-Liquid Systems [in Russian], Moscow (1976).
2. G. Wallace, One-Dimensional Two-Phase Flows [Russian translation], Moscow (1972).
3. J. Hewitt and N. Hall-Taylor, Annular Two-Phase Flows [Russian translation], Moscow (1974).
4. V. A. Mamaev, G. E. Odishariya, O. V. Klapchuk, et al., Motion of Gas-Liquid Mixtures in Pipes [in Russian], Moscow (1978).
5. M. N. Kemel'man, Linear Vapor Separation and New Means to Raise Its Efficiency [in Russian], Diss. Kand. Tekh. Nauk, Moscow (1957).
6. N. A. Mozharov, Teploenergetika, No. 2, 50-53 (1959).
7. N. A. Mozharov, Teploenergetika, No. 4, 60-63 (1961).
8. S. S. Kutateladze and Yu. L. Sorokin, "Questions of heat elimination and hydraulics of two-phase systems," Coll. Sci. Work [in Russian], 315-324, Moscow (1961).
9. Yu. L. Sorokin, Trudy, Tsentr. Kotel. Tekh. Inst., No. 59, 129-135 (1965).
10. O. L. Pushkina and Yu. L. Sorokin, Trudy, Tsentr. Kotel. Tekh. Inst., No. 96, 34-39 (1969).
11. Yu. L. Sorokin, A. G. Kiryashkin, and B. G. Pokusaev, Khim. Neftyan. Mashinostr., No. 5, 35-38 (1965).
12. Yu. L. Sorokin, Prikl. Mekh. Tekh. Fiz., No. 6, 160-165 (1963).
13. I. I. Sagan', N. Yu. Tobilevich, S. I. Tkachenko, et al., Izv. Vyssh. Uchebn. Zaved., Energetika, No. 12, 69-72 (1969).
14. L. Ya. Zhivaikin, Khim. Mashinostroenie, No. 6, 25-29 (1961).
15. B. I. Nigmatullin, V. I. Rachkov, and Yu. Z. Shugaev, Teploenergetika, No. 6, 51-55 (1980).
16. A. M. Podsushnyi, V. V. Permyakov, B. Ya. Karastelev, et al., Temperature Mode and Hydraulics of Vapor Generators [in Russian], Coll. Sci. Work, 238-242, Leningrad (1978).
17. A. N. Butenko, A. E. Potapenko, and E. S. Chistyakov, Gas Thermodynamics of Multiphase Flows in Power Plants [in Russian], No. 1, 86-91, Khar'kov (1978).
18. M. K. Bezrodnyi, Inzh.-Fiz. Zh., 34, No. 6, 1001-1006 (1978).
19. M. K. Bezrodnyi, Boiling and Condensation [in Russian], 59-68, Riga (1982).